The 15th International Symposium on Magnetic Bearings, August 3-6, 2016, Mojiko Hotel, Kitakyushu, Japan

ISMB15

Automated Design of AMB Rotor Systems with Standard Drive, Control Software and Hardware Technologies

Rafal P. JASTRZEBSKI*,[a], Teemu SILLANPAA*,[b], Pekko JAATINEN*,[c], Alexander SMIRNOV*,[d], Jouni VUOJOLAINEN*,[e], Tuomo LINDH*,[f], Antti LAIHO**,[g], Olli PYRHÖNEN*,[h]

*Dept. of Electrical Engineering, Lappeenranta University of Technology, 53851 Lappeenranta, Finland

**ABB, Oy Motors and Generators, Helsinki, Finland

E-mail: [a]Rafal.Jastrzebski@lut.fi, [b]Teemu.Sillanpaa@lut.fi, [c]Pekko.Jaatinen@lut.fi, [d]Alexander.Smirnov@lut.fi, [e]Jouni.Vuojolainen@lut.fi [f]Tuomo.Lindh@lut.fi, [g]Antti.Laiho@fi.abb.com, [h]Olli.Pyrhonen@lut.fi

Abstract

Industrial applications of active magnetic bearings (AMBs) technology have been continuing to grow for over 4 decades. However, the volume and cost reduction for consumer products are still lower than industrial potential. Particularly, bearing design to match the application, control design, commissioning, control tuning, electronics design and scaling of VA rating to match the bearings make the significant contribution to overall cost of new AMBs. This paper describes how to design and implement an industrial 5 degrees of freedom AMB suspension and model-based control for rotating systems quickly and efficiently. The presented solution leverages the existing commercialized drives and automation components for making the AMB products. With the automated analytical design of AMB actuators and control in respect to design constrains the design & engineering of the product are completed. This leads to easier scalability, standardization, lead-time reduction, and broadening the application area.

Keywords: Standard drive hardware, Digital control design, System identification, Active magnetic bearing, High-speed motor, Induction motor, Magnetic levitation

1. Introduction

The classical active magnetic bearing (AMB) technology has long matured with advances of solid-state electronics and digital control technology e.g. (Habermann and Liard, 1979), (Schweitzer, 1976). However, high cost of customized hardware and control software has limited the application growth and wider industrialization. Typically, established AMB suppliers develop their own distinct solutions for electronics (Swann, 2014), (Kumar and Jayawant, 2014), which leads to challenges in standardization, scalability and cost reduction for newcomers.

Yet the AMB system building blocks are very similar to standard motor components making the technology potentially widely applicable and very affordable. Recently, many teams have tried to increase AMB system reliability and decrease cost and time to market by replacing custom electronics with the more standard components (Yim, et al., 2008), (Ahn, 2011), (Denk, et al., 2012), (Denk, et al., 2013). Still, hardware design, control software commissioning, identification and design tuning are not available for customers who would like to use the AMBs in their applications but who are lacking the technology in-depth knowhow. In order to gain customer confidence various application specific requirements of AMB control (Swanson, et al., 2014) have to be fulfilled. In order to extend the application area and gain the market share further an over-all system cost and lead time have to be decreased.

AMB supported motor and generator applications are usually series products with little product variations. Developing of such products allows limited designing costs. The AMB design flow is a complex task comprising of mechanical load calculus, rotor dynamics calculus, electromagnet design of actuators, plant modelling, control design, and driver selection. Plant modeling, controller design and testing are iterative tasks that have to account for uncertainties. Closed-loop commissioning and identification require stable initial AMB control under the presence of disturbance forces from a machine axle, unbalance, drive disturbances, motor pull, sensor runouts, signal noise and biasing. A few manufacturers already offer AMB actuators as catalog products. Our focus is on developing design and commissioning chain that would help in dimensioning and implementation of such products.

The paper summarizes a decade of AMB technical development at Lappeenranta University of Technology (LUT) from the preparation for industrialization perspective. First, we introduce automated engineering tools. The AMB design flow tools comprise an electromagnet design, control design and driver selection. The initial controller is automatically synthetized based on a rigid rotor model, generated AMB models and selected performance. Second, we present case study prototype followed by an overall control system layout comprising standard drive and automation hardware. Different options for the proximity sensors selection including a custom low-cost integrated LUT designed sensors are presented. Third, we reveal the controller implementation in standard automation PC/PLC-based platform. Finally, an industrial 350 kW 15000 r/min induction motor is equipped with designed proof of concept AMBs. We present laboratory measurements that show the prototype operation. The final model-based controller includes the bending modes of the AMB rotor system as state variables. The final controller tuning uses results of complementing commissioning and identification tools.

2. Automated engineering tools and design flow

The design tool chain (Fig. 1) provides the analytical dimensioning of the AMB system based on requirements of application. The requirements include motor power, motor rotational speed, mass distribution to bearings, space, material and thermal constraints, and expected disturbance forces and their acting planes in respect to the rotor.

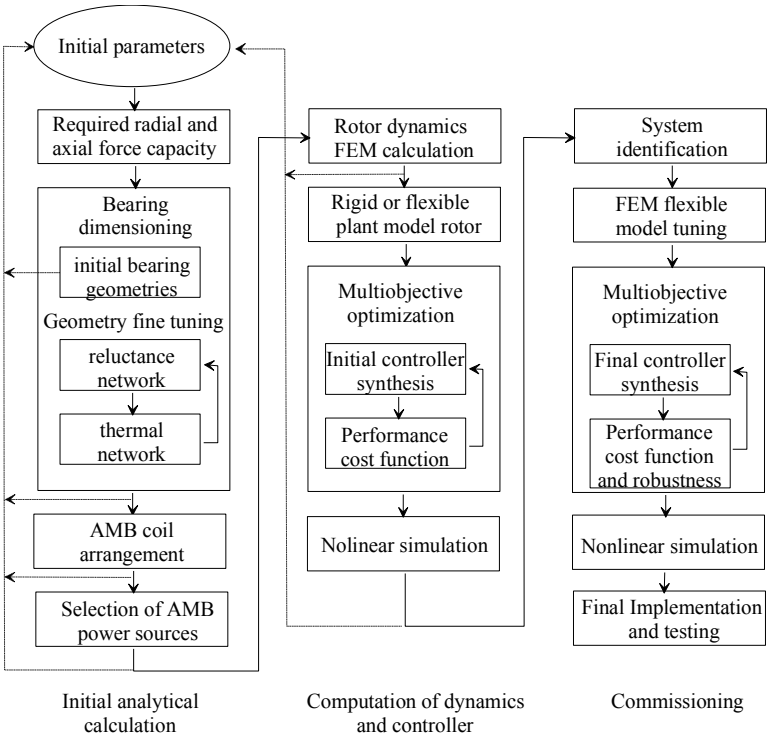

Fig. 1 Design tool chain.

In the first analytical calculation phase, radial and axial force estimation is made. All the expected forces from mass distribution, external forces, e.g. compressor wheel pull and unbalanced pull of rotor are summed up and averaged and maximum bearing forces as well as slew rate of forces that bearings should be able to produce are determined. The geometric and electrical properties of bearings can be refined iteratively using a reluctance network method and a thermal network model (Pöllänen et al., 2006). Coil area arrangement is optimized for selected AMB geometry. Initial values for current stiffness and position stiffness are obtained. The geometric properties of bearings may or may not require changes in initial mechanical dimensioning of the machine. In this phase, if bearings do not fit to original mechanical design, the mass of rotor as well as locations of bearings may change and the first calculation phase is repeated. Suitable power sources are selected.

In the second phase, initial FEM rotor dynamic calculations and initial controller synthesis are performed. If only the mass, length and locations of actuators and sensors are available the rigid body model is used. Otherwise a detailed

rotor dynamics calculation is computed resulting in information of probable mode shapes and corresponding critical frequencies. In this phase, in the case of over-critical rotor, the locations of bearings and sensors are changed. The rigid body model-based multi-input multi-output (MIMO) control is tuned with multi-objective optimization. Alternatively, a decentralized controller where every bearing axis has own independent control is applicable (Jastrzebski and Pöllänen, 2009b). Jastrzebski and Pöllänen, (2009b) describe the benefits of model based MIMO control over classical decentralized control approaches. For gyroscopic systems, the gain scheduling (Jastrzebski, et al., 2010a) or linear parameter-varying approaches (Smirnov et al., 2010) can be applied. A nonlinear plant model comprising AMB models and rotor model is constructed, The controller performance and robustness during initial lift up, disturbance force reference, unbalance, and noise conditions are tested in nonlinear simulations. The iterations with the first phase can take place if the satisfactory performance cannot be achieved. As a result, a control system can be built and the controller can be implemented.

In the commissioning phase, a system identification procedure is used for correction of initial calculated models. First, the sensors are auto-calibrated and amplifiers are pre-tested (Smirnov, 2012). Second, the frequency domain identification, such as stepped sine, broadband (Hynynen, 2011) or pseudorandom binary sequence (PRBS) methods can be applied. The PRBS methods yield the fastest identification times and are most robust, while stepped sine methods can provide the best signal to noise ratio at higher frequencies. The FEM flexible rotor model and the actuator dynamical models are updated. The final model-based MIMO controller that includes identified bending rotor modes is synthesized. In the final testing phase, the updated controller is verified with the customer machine.

2.1 Dimensioning of magnetic bearings based on the required supporting forces

The geometry of radial bearings is defined by the maximum and average force constraints. Based on the maximum force and selected maximum flux density in the airgap it is possible to estimate the necessary surface area of the poles. In the symmetrical case, which is beneficial in most industrial products, the maximum force should be applied in all possible directions. For force capacity, a reduction coefficient σ is introduced to take into account the selected actuator geometry (Fig. 2) and current control. From the geometrical dimensions the effective pole area is defined as

$$A = 2(r_j + g_0) l_j \sin(\frac{\pi f_i}{n}), \tag{1}$$

where r_j is the radius of the bearing journal, n is the number of poles, g_0 is the airgap width, l_j is length of the journal f_i is iron ratio that denotes the relation between total circumferential length and length occupied by the poles. The necessary pole area to provide the maximum force f_{max} is defined as follows

$$A = \frac{f_{max}\mu_0}{B_{sat}^2 \sigma}, \tag{2}$$

where B_{sat} is saturation flux density selected based on material properties, μ_0 is permeability of vacuum. For bearing design a journal radius or rotor radius is specified. The necessary journal width is defined as equal to the width of the pole $w_j = w = A/l_j$ and thus the rotor radius r_r and journal radius r_j are related $r_j = r_r + w_j$. Combining equations (1)-(2) and substituting journal or rotor radius the basic geometry of bearing is established.

Next step is estimation of bearing stator geometry. Width of the pole is assumed equal to the journal width and the stator yoke. The length of pole is defined by the space necessary for windings. The surface area of winding is defined by the thermal stability of the system so that coils are not overheated when system supplies average force

$$N i_{RMS} \leq J_{RMS} A_c f_c, \tag{3}$$

where N stands for the number of coil turns, i_{RMS} is average current, A_c denotes the coil area, J_{RMS} is average current density and f_c is copper packaging factor. With air cooling the current density is 5 A/mm^2. The coil packaging factor depends on manufacturing processes and its value is about 0.5. The poles insulation and space reduction can be taken into account in packaging factor. For removable coils the available area is estimated as follows

$$A_c = \left((r_j + g_0)\tan\frac{\pi}{n} - \frac{w}{2}\right)(r_y - r_j - g_0), \tag{4}$$

where r_y is the inner radius of stator yoke.

With the presented equations and workflow the geometry of radial heteropolar bearing without flux splitting is estimated. The equations do not take into account flux leakages, flux fringing in the airgap and magnetomotive force for

the iron parts. For geometry fine-tuning, a reluctance network method is utilized which provides accuracy close to the accuracy of FEM with much shorter calculation time (Romanenko et al., 2014).

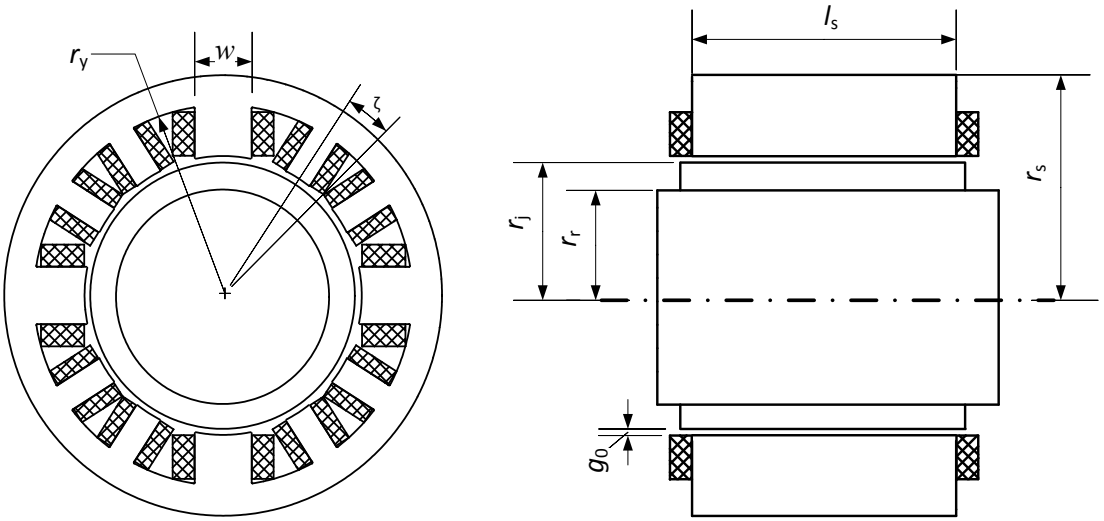

Fig. 2 Radial bearing cross section and its main dimensions. E-core structure provides the flux splitting in the journal and in the yoke. The main benefit is reduced journal dimension, more even flux distribution and reduced losses.

The E-core geometry can be calculated with the same workflow presented above under assumption that number of poles is eight. It is valid when width of the small pole is half of the big pole and journal width is half of the middle pole width. The side poles locations are defined by the angle ζ. Therefore, the area of small coil is defined as

$$A_{c,s} = \left(\left(r_j + g_0 \right) \tan \zeta - \frac{w_j}{2} \right) \left(r_y - r_j - g_0 \right). \tag{5}$$

Simultaneous optimization of equations (4) and (5) to achieve the necessary flux and satisfy the geometry constraints leads to the final solution.

2.2 Designing of model-based multi-input multi-output robust control

We assume general AMB rotor system comprising two radial AMBs, one axial AMB, and single motor in between the radial bearings. This plant can be modeled as a linear and time-invariant system. For the linear controller synthesis, the tools construct three plant models. The first model is used for the construction of the estimator and linear feedback. For the initial controller it only comprises the rigid body model and basic actuator dynamics; while for the final controller it is typically sufficient to include the first bending mode (for subcritical rotor). The second, higher order, model features flexible FEM based rotor model and optionally uncertainties (Jastrzebski et al., 2010a); and it is meant for the control synthesis verification in the single- (multi) objective tuning procedure. The third, the most detailed, model comprises nonlinear actuator models, sensor and transportation delays and disturbances. The third model is used in the final stage of the controller verification in Matlab/Simulink® simulations. For the plants with a decoupled radial and axial suspension, the open-loop transfer function of the (radial) plant in the Laplace domain is

$$\boldsymbol{y} = \boldsymbol{G}(s)\boldsymbol{u} = \boldsymbol{C}(s\boldsymbol{I} - \boldsymbol{A})^{-1}\boldsymbol{B}\boldsymbol{u}, \tag{6}$$

For the current controlled AMBs $\boldsymbol{u}$ and $\boldsymbol{y}$ are the vectors of the input control currents and the output measured displacements, respectively. $\boldsymbol{G}$(s) is a 4×4 transfer function matrix of the plant, where $\boldsymbol{A}$, $\boldsymbol{B}$ and $\boldsymbol{C}$ are the state matrix, the output matrix and the input matrix, respectively.

With the control plant models, different MIMO type controllers for AMBs including LQG and H_∞ types can be applied (Jastrzebski and Pöllänen, 2008), (Jastrzebski, 2009a), (Smirnov and Jastrzebski, 2009) and (Jastrzebski, et al., 2010a, 2011). The robust controllers require casting the problem into a general control configuration and solving γ-iterations. For the LQG controllers the weighting functions are scalar matrices. For the H_∞ controllers the first and second order weighing functions are sufficient in most cases. The control tuning is performed either by selecting the weighting functions manually (or using predefined weighting functions) or using multi-objective tuning, e.g. a differential evolution

approach and a predefined cost function. Based on the plant model characteristics the suitable cost function parameters are selected which are desired bandwidth, maximum input and output sensitivity peaks and sensitivity to the selected disturbances as well as time responses to reference inputs and disturbances. For example, in the case of a single objective genetic algorithm optimization all sub- cost functions (e.g. different sensitivity peaks and maximum amplitudes of responses) can be combined into a single cost function as a weighted sum. In the multi-objective case, a solution from a Pareto optimum front is selected (Smirnov and Jastrzebski, 2009).

Based on the synthetized controller the tools propose to the user the specific standard ABB drives required for the AMB current source realization for the levitation support of the case study customer machine.

3. Case study AMB design example for high-speed drive

The electrical machine under discussion is a solid rotor induction machine. Induction machines have robust and reliable structure. The solid rotor allows reaching high surface speeds without adding flexibility. This alleviates rotor dynamics issues when flexible modes are close to the operation region. Induction machines are usually characterized by low power factor that requires oversized inverter for operation and as a result increased price of the unit. To increase the power factor the rotor is slitted. This directs the flux deeper into the rotor medium and in addition decreases the conductivity of the rotor surface, which increases not only the power factor but also the efficiency. The other measure to improve efficiency is an attachment of end-rings to the active rotor parts. The end-rings are made from high conducting material also decreasing conductivity of the rotor active surface. Figure 3 presents the case study machine that has 350 kW power at nominal point of 15000 rpm with power factor more than 0.7. Figure 4 shows the rotor cross section, as in FEM used in the control verification, and the first four rotor bending modes.

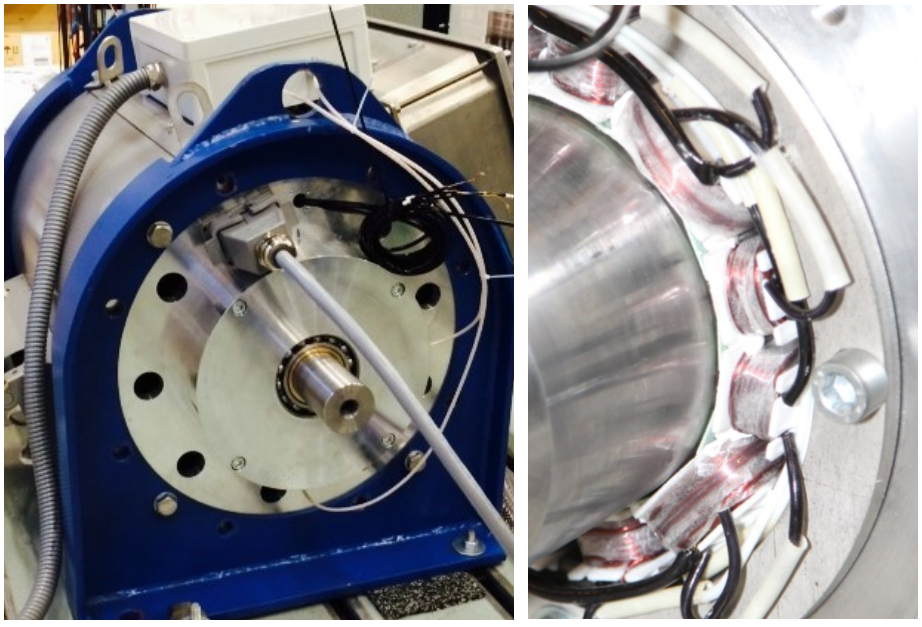

(a) (b)

Fig. 3 (a) Proof of concept high-speed 350 kW 15000 r/min electrical machine. (b) Designed AMBs

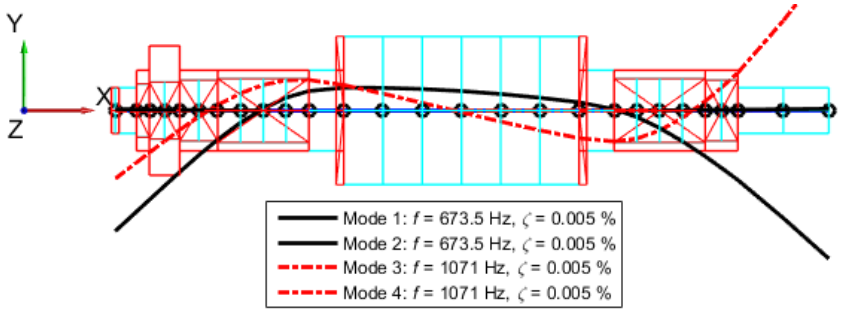

Fig. 4 Finite element model of the rotor and shape of two free-free modes

4. Industrial components for AMB system

The position control layer is implemented using Beckhoff TwinCAT environment running in a Beckhoff Industrial PC (Fig. 5). With the EtherCAT fieldbus connection provided by the platform, the position control layer can connect to any industrial EtherCAT-enabled automation system using standard fieldbus communication with cycle times as short as 50 µs and I/O response times from 85 µs. The communication delays and measurement noise in the system can be minimized by elimination of analog signal paths. The analog input signals can be oversampled to the fieldbus with higher rate than the cycle time, with sampling rates up to 100 kHz using commercial EtherCAT based analog input modules. (Beckhoff Automation, 2007).

The position control layer was constructed using model-based design methodology within the MATLAB/Simulink allowing rapid development, simulation, system verification and automatic code generation. The tuned controllers can be loaded to predefined framework. The Beckhoff TwinCAT runtime environment running on the industrial PC hardware allows real-time control algorithms implemented using an international electrotechnical commission (IEC) 61131 standard programming languages, C-routines as well as Simulink generated modules. If required, the control algorithms and structure can be easily changed. For example, nonlinearity compensation can be added for systems with a low bias (Jastrzebski, et al., 2014b).

The standard industrial drive modules driving the magnetic bearing coils were equipped with a custom modulator and current controller connected to the EtherCAT fieldbus. The modern standard industrial frequency converter hardware fulfills the needs of the magnetic bearing control system as a current source. With small software modifications in the modulator part the drive is able to use the three phase bridge to drive two winding load consisting of a one control axis of the AMB system (Holmes and Kotsopoulos, 1993), (Yim, et al., 2002).

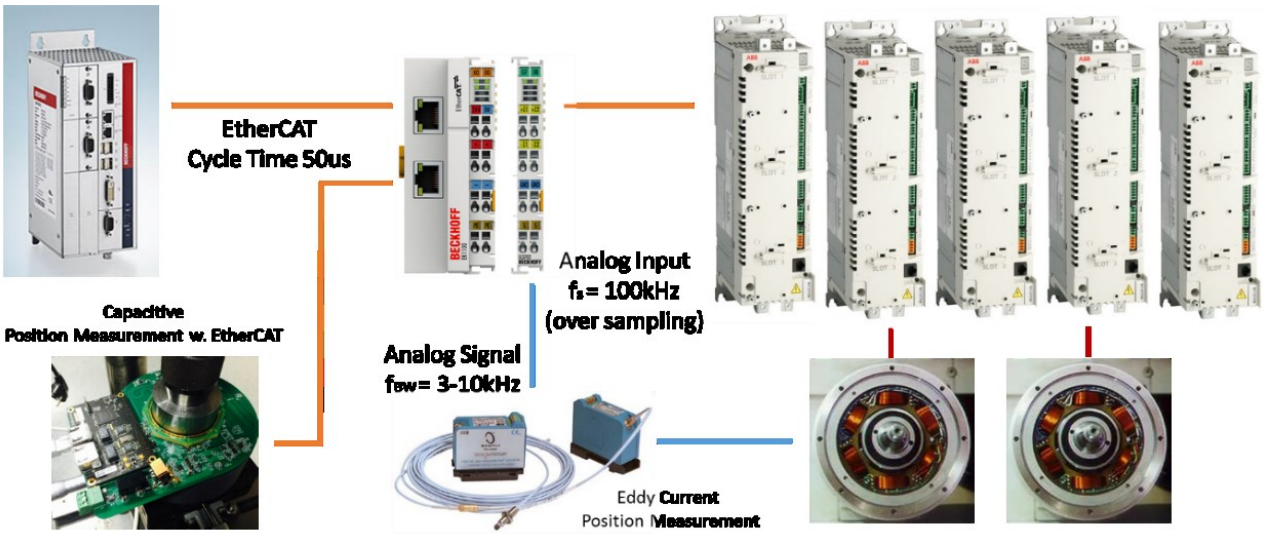

Fig. 5 Industrial PC and EtherCAT based control system of the proof of concept AMB solution. Various sensors including standard eddy current proximity sensors with an analog input, low-cost integrated eddy-current sensors (Jastrzebski et al., 2010b) or the low-cost/high bandwidth sensors with integrated ADCs and EtherCAT outputs (Jastrzebski, et al., 2014a) can be connected.

5. Measurements and commissioning with proof of concept induction motor prototype

The industrial electrical machine has been retrofitted with the designed AMBs. Magnetic center calibration of the rotor was implemented and performed using Beckhoff PLC and Simulink® models. The magnetic center point is assumed to correspond to the plant linearization point, where the force availability is maximized in all radial directions. This makes the magnetic center an ideal operating point of the system. Magnetic center calibration was repeated 5 times and the average value of these repetitions was used as a reference operation point. The magnetic center of the rotor is located approximately at (70.7, 10.49, 148.66, -20.65) µm from the geometric center (detected as a results of the clearance test).

Figure 6a shows the result of the magnetic center calibration. Dots in the figure indicate a separate repetition and X shows the average value (magnetic center location).

The frequency domain identification with step-sine excitation and adaptive amplitude selection was implemented and performed using Beckhoff PLC and Simulink® models. Amplitude limit was 2.5 A and the frequency range was from 1 Hz to 750 Hz in 3.01 Hz steps. Results of the step-sine identification on Ax-axis are shown in Fig. 6b.

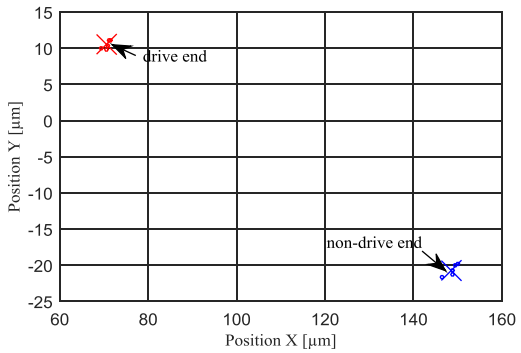

Fig. 6 (a) Determination of magnetic center of the rotor for drive and non-drive end. Dots show the separate repetitions and X shows the location of the magnetic center.

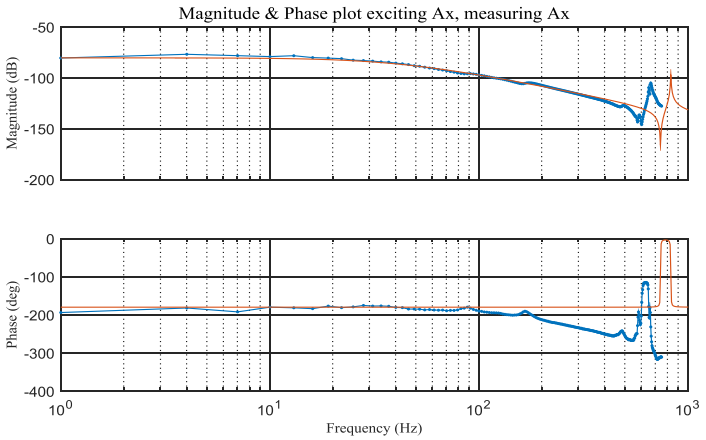

Fig. 6 (b) Results of the step-sine identification compared to the initial FEM results on Ax-axis. Blue line is the experimental data and the orange line is the initial FEM result.

Conclusions

Design and implementation of AMB solution for industrial drives require feasible design procedure and cost competitive implementation using standard industrial components. The design procedure can take advantage of modern computer tools, where rotor dynamics, actuator electromagnetic dimensioning and AMB control synthesis can be analyzed and developed by following systematic design rules. The same design environment can be used to analyze the system dynamics and fine-tune the controller. System unidealities, like measurement noise, control loop delays, rotor unbalance, motor magnetic pull, AMB actuator magnetic saturation and force nonlinearity can be taken into account by careful system modelling and simulations. By using standard industrial components, like PLC technology for control algorithms and industrial drive modules as current amplifiers, a cost competitive implementation is achievable. Additional benefit of PLCs is a standard programming environment also for other control, monitoring and communication purposes. AMB tailored position measurement system has potential to reduce further the system costs. Effective design procedure combined with system solution based on standard industrial components and feasible position measurement makes AMB technology affordable for wider scale of industrial applications.

Acknowledgment

The authors would like to express their gratitude to ABB Oy Motors and Generators for their financial support. The work has been co-funded by Academy of Finland No. 270012 and No. 273489.

References

Ahn, H., Dynamic performance limitation in driving a radial AMB with space vector PWM, in Proc. of 11th International Symposium on Magnetic Bearings (ISMB 11) (2008), pp.54–61.

Beckhoff Automation GmbH & Co. KG, XFC – eXtreme Fast Control Technology, Application Note (2007).

Denk, J., Köpken, H.-G., Stoiber, D. and Viering, F., Active magnetic bearing systems for turbomachinery applications based on standard drive technology, in Proc. of 13th International Symposium on Magnetic Bearings (ISMB 13) (2012), pp.1–16.

Denk, J., Stoiber, D., Köpken, H.-G. and Walter, H., Industrialization of AMB Systems with Standard Drive Technology,

IEEE Transanctions on Industry Applications, Vol.49, No.2 (2013), pp.791–798.
Habermann, H. and Liard, G., Control: practical magnetic bearings: electronically controlled electromagnets support spinning 1100-kg shafts to micrometer accuracy, IEEE Spectrum, Vol.16, No.9 (1979), pp. 26–30.
Holmes, D.G., Kotsopoulos, A., Variable speed control of single and two phase induction motors using a three phase voltage source inverter, in Proc. of Conference Record of the IEEE Industry Applications Society Annual Meeting (1993), pp. 613–620.
Hynynen, K., Broadband Excitation in the System Identification of Active Magnetic Bearing Rotor Systems, Dissertation, Acta Universitatis Lappeenrantaensis 446, LUT, Finland, (2011).
Jastrzebski, R.P. and Pöllänen, R., Trade offs in LQ/LTR control designs for MIMO AMB systems, in Proc. of 11th International Symposium on Magnetic Bearings (ISMB 11), (2008), pp. 433–440.
Jastrzebski, R.P., Signal-based H_∞ optimal control for AMB system based on genetic algorithm, in Proc. of IEEE International Conference on Control and Automation, (2009a), pp. 715–721.
Jastrzebski, R.P., and Pöllänen, R., Centralized Optimal Position Control for Active Magnetic Bearings – Comparison with Decentralized Control, Electrical Engineering, Vol. 91, No. 2, (2009b), pp. 101–114.
Jastrzebski, R.P., Hynynen, K. M. Smirnov, A., H_∞ control of active magnetic suspension, Mechanical Systems and Signal Processing, Vol. 24, Issue 4, (2010a), pp. 995–1006.
Jastrzebski, R.P., Tolsa, K. and Iskanius, M., Customization of digital circuit for material–independent eddy current proximity sensor for active magnetic bearings, In Proc. of 12th International Symposium on Magnetic Bearings (ISMB 12), (2010b), pp. 376–382.
Jastrzebski, R.P., Smirnov, A. Pyrhönen, O. and Piłat, A. K., Discussion on Robust Control Applied to Active Magnetic Bearing Rotor System, Challenges and Paradigms in Applied Robust Control, (2011).
Jastrzebski, R.P., Matusiak, D., Sillanpää, T., Romanenko, A., Jaatinen, P., Tolsa, K., Lindh, T. and Pyrhönen, O., Modelling and evaluation of radial-axial PCB capacitive position sensor prototype, in Proc. of 16th European Conference on Power Electronics and Applications (EPE'14-ECCE Europe) (2014a), pp. 1–8.
Jastrzebski, R.P., Smirnov, A., Mystkowski, A. and Pyrhönen, O., Cascaded position-flux controller for an AMB system operating at zero bias, Energies 2014, Vol.7, No. 6 (2014b), pp. 3561–3575.
Smirnov A. and Jastrzebski, R.P. Differential evolution approach for tuning an H_∞ controller in AMB systems, in Proc. of 35th Annual Conference of IEEE Industrial Electronics, (2009), pp. 1514–1518.
Kumar, P. and Jayawant, R., Design synthesis and experimental validation of an AMB controller with a power dense amplifier for retrofit applications, in Proc. of 14th International Symposium on Magnetic Bearings (ISMB 14) (2014), pp. 627–632.
Pöllänen, R., Nerg, J., Rilla, M. and Pyrhönen, O., Transient Thermal Model for Radial Active Magnetic Bearing", In Proc. of 10th International Symposium on Magnetic Bearings (ISMB 10), (2006).
Romanenko, A., Smirnov, A., Jastrzebski, R.P. and Pyrhönen, O., Losses estimation and modelling in active magnetic bearings, in Proc. of 16th European Conference on Power Electronics and Applications (EPE'14-ECCE Europe) (2014), pp. 1–8.
Schweitzer, G., Characteristics of a magnetic rotor bearing for active vibration control, in Proc. of First International Conference on Vibrations in Rotating Machinery (1976), Paper C239/76.
Smirnov A. and Jastrzebski, R.P. Differential evolution approach for tuning an H_∞ controller in AMB systems, in Proc. of 35th Annual Conference of IEEE Industrial Electronics (2009), pp. 1514–1518.
Smirnov, A. and Jastrzebski, R.P. and Hynynen, K., Gain-scheduled and linear parameter-varying approaches in control of an active magnetic bearings, In Proc. of ISMB 12 (2010), pp. 350–360.
Smirnov, A., AMB System for High-Speed Motors Using Automatic Commissioning, Dissertation, Acta Universitatis Lappeenrantaensis 508, LUT, Finland, (2012).
Swann, M.K., Industrialisation trends for active magnetic bearings in the turbomachinery industry, in Proc. of 14th International Symposium on Magnetic Bearings (ISMB 14) (2014), p. 828.
Swanson, E., Hawkins, L., and Masala, A., New active magnetic bearing requirements for compressors in API 617 eighth edition, In Proc. of 43rd Turbomachinery Symposium (2014).
Yim, J.S., Kim, J.H., Sul, S.K., Ahn, H.J., Park, I.H., Han, D.C. and Choi, S.H., A novel cost-effective scheme of power amplifier for AMB using space vector technology, in Proc. of 8th International Symposium on Magnetic Bearings (ISMB 8) (2002), pp. 101–106.